

A process-based model for spatial interpolation of extreme temperatures and solar radiation

G. A. Baigorria¹ and W. T. Bowen²

Abstract

In mountain areas there is a high variability in microclimates at relatively short distances, caused by the complex terrain and the low water vapor content in the atmosphere due to the high altitude. In addition, scarcity of weather stations and the inadequate availability of temporal information restrict the possibility of accurately depicting real variations. Many models have been developed for climatic interpolation, but their usefulness is limited if the variables causing the spatial variation (e.g. topography) are not included. A process-based model for interpolating maximum and minimum temperatures and solar radiation in complex mountainous terrain was developed. The model is based on the observation that net radiation is zero twice in a day, just when extreme temperatures occur. These temperatures are taken from on-site observations; therefore, the atmospheric conditions estimated at these moments are known and incorporated as constant values in the model. The simulation of the state of the atmosphere on a daily basis is thus feasible generating the data needed for the spatial interpolation of the extreme temperatures. The topographic variables altitude, slope, and aspect as derived from a digital elevation model (DEM) are also included in the model. The resolution of resulting maps in raster format is controlled by the resolution of the DEM. The extreme temperature maps were used as input into the calibrated model for estimating the daily total solar radiation. Validation was made comparing the observed data from control weather stations versus the model-estimated point data. The model was developed and tested in two adjacent watersheds in the northern Andean mountains of Peru.

INTRODUCTION

Spatial distribution estimates of meteorological data are becoming increasingly important as inputs to spatially explicit landscape, regional, and global models. Spatial interpolation is especially important in mountainous regions where data collection is sparse and variables may change over short distances. Interpolation techniques have been developed to estimate meteorological variables over a

landscape, but often their usefulness is limited because variables that cause the spatial variation (e.g., topography) are not included. Process-based models for interpolation differ from their geostatistical counterparts in that they are constructed primarily from knowledge or understanding of the processes that produce the spatial variation. The mathematical form of the process-based models arises mainly from an understanding of processes rather than from statistical relationships (Willmott 1996).

¹ International Potato Center (CIP), P.O. Box 1558, Lima 12, Peru. E-mail: g.baigorria@cgiar.org

² CIP-Quito/IFDC, P.O. Box 17-21-1977, Quito, Ecuador

The research reported here concerns the development of an interpolation technique for estimating maximum and minimum temperatures and solar radiation in mountainous terrain. The technique incorporates topographic information on altitude, aspect, and slope provided by a digital elevation model (DEM). In addition, software has been developed that links the interpolation model to a GIS. An application of the climate interpolator is demonstrated for two adjacent watersheds in the northern Andes of Peru.

MATERIALS AND METHODS

Model Development

A model, Climate Interpolator, was developed based on the relationships described below in the Model Formulae section. To interpolate monthly microclimate conditions in mountainous terrain, Climate Interpolator requires inputs of site-specific monthly values for minimum and maximum temperatures and solar radiation. The exact location of the weather stations is also needed. The model then provides monthly GIS layers of the same variables interpolated using the resolution of the DEM.

Many processes in the atmosphere depend on the net flux of radiation at the earth's surface resulting from the balance between the solar (short-wave) and terrestrial (long-wave; $LW \uparrow$) fluxes. Daily processes of warming and cooling depend on this balance, which is negative during the night and positive during the day. Therefore, net flux of radiation (NR; difference between short-wave solar and long-wave terrestrial fluxes) is zero twice in a day, just when extreme temperatures occur (Figure 1). The simple relationships shown in Figure 1 provide the framework for interpolating temperature extremes and solar radiation across the landscape.

The short-wave and $LW \uparrow$ radiation balance can be calculated directly and indirectly, respectively, at points where weather stations are measuring incoming short-wave solar radiation (direct and diffuse) with pyranometers. While the pyranometer provides an estimate of the short-wave radiation, the Stefan-Boltzmann law is used to calculate $LW \uparrow$. Long-wave atmospheric radiation ($LW \downarrow$) is also calculated using the relationship shown in Figure 1.

With $LW \downarrow$ calculated, and with the atmospheric transmission coefficient (τ) also calculated, it is possible to estimate the maximum and minimum

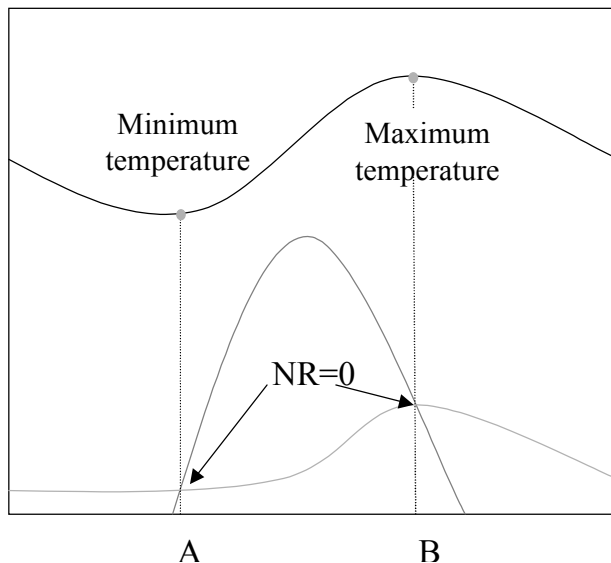


Figure 1. Hourly distribution of temperature (—), short-wave balance (---), and long-wave balance (· · ·). NR = net radiation. “A” is the time minimum temperature occurs (approximately one hour before sunrise) and “B” is the time maximum temperature occurs (approximately 14:00 hours).

temperatures for each point of a grid in a raster format. These temperatures are calculated according to the topography and net radiation; these same data are then used to estimate daily solar radiation for each point of the grid using an empirical equation for the area under study. All calculations are described in more detail in the section on interpolation formulas.

The Climate Interpolator model was developed, parameterized, and tested using data collected in two adjacent watersheds (La Encañada and Tambomayo) located near Cajamarca in the northern Andes of Peru. The software system is based on a DEM (elevation, slope, and aspect) that partitions the area into a grid of 628 x 482 cells with an individual cell size of 30 x 30 m.

The meteorological information is specified in the model according to the standards set by the International Consortium for Agricultural Systems Applications (ICASA; Hunt and Boote 1998). The model is considered a prototype in need of yet more rigorous testing of some subroutines (e.g. surface temperature calculation and auto calibration of the incoming solar radiation calculation). The next step of ongoing research will be to generate daily GIS layers of weather variables for driving plant and soil models.

Model formulae

Calibration of atmospheric conditions

For each weather station, daily values for solar radiation, minimum temperature, and maximum temperature were recorded. With this information, transmissivity of the atmosphere (τ) and long-wave atmospheric radiation ($LW \downarrow$) were calculated for each location. The atmospheric transmission coefficient (τ) is the ratio between intensity of the incoming radiation at the earth's surface measured by pyranometers, $(Q + q)_i$, and the extraterrestrial radiation Q_t (radiation intensity just outside the atmosphere):

$$\tau = (Q + q)_i / Q_t \quad (1)$$

where τ is dependent on clouds (amount and type) and other scattering components (dust, CO_2 , etc.). For clear skies in mountainous areas a transmission coefficient of 0.9 is common (Lee, 1978). Q_t is dependent on latitude (ϕ) and the solar constant (S ; $cal\ cm^{-2}\ min^{-1}$) (Hartkamp, 1995):

$$S = 1.9613 \times [1 + 0.33 \times \cos(2\pi \times (\text{DayOfYear} - 10) / 365)] \quad (2)$$

Earth-Sun distance is calculated as (García, 1994),

$$(dm/d)^2 = C1 + C2 \times \cos(\theta) + C3 \times \sin(\theta) + C4 \times \cos(2\theta) + C5 \times \sin(2\theta) \quad (3)$$

where $C1 = 1.00011$, $C2 = 3.3523 \times 10^2$, $C3 = 1.28 \times 10^3$, $C4 = 7.39 \times 10^4$, $C5 = 9.9 \times 10^5$ and;

$$\theta = (2\pi \times \text{DayOfYear} / 365) \quad (\text{as radians}) \quad (4)$$

Solar declination is given by (García, 1994):

$$\delta = -23.45^\circ \times \cos(n \times 360 / 365) \quad (\text{as degrees}) \quad (5)$$

where n is the number of days from 22 December ($n=0$). The hour angle (H) at sunset and sunrise (Bonan 1989):

$$H = \text{ArcCos}[-\tan(\phi) \times \tan(\delta)] \quad (6)$$

To find the value of long-wave atmospheric radiation ($LW \downarrow$) it was necessary to consider the time when the Net Radiation (NR) is zero twice a day (just when the extreme temperatures occur). Minimum

temperature occurs around an hour before sunrise and the maximum temperature usually occurs two hours after noon. With these moments located, $LW \downarrow$ is calculated for each time with the equation:

$$NR = (Q + q)_i \times (1 - \alpha) - LW \uparrow + LW \downarrow = 0 \quad (7)$$

where α is the surface albedo, and $LW \uparrow$ is the long-wave terrestrial radiation calculated by the Stefan-Boltzmann law (Peixoto and Oort, 1992).

$$LW \uparrow = \epsilon \sigma T^4 \quad (8)$$

where ϵ is emissivity, σ is the Stefan-Boltzmann constant ($8.13486 \times 10^{-11}\ cal\ cm^{-2}\ min^{-1}\ K^{-4}$), and T the surface temperature (Kelvin).

In addition, it is necessary to disaggregate direct (Q_i) and diffuse (q_i) radiation to include the effects of topographic parameters—slope and aspect—on the direct radiation. This effect was measured by (García, 1994):

$$Q_i = S \times Dm \times \left[\begin{array}{l} \cos(Z) \times \cos(\text{Slope}) + \\ + \sin(Z) \times \sin(\text{Slope}) \times \cos(a - a') \end{array} \right] \quad (9)$$

where Q_i ($cal\ cm^{-2}\ min^{-1}$) is the direct solar radiation on a slope surface with $\tau = 1$, Z is the zenith angle (equation 10), a is the sun azimuth angle (equation 12), and a' the wall azimuth angle, which is the aspect of the slope from the south (Keith and Kreider, 1978).

$$Z = \text{ArcCos}[\sin(\phi) \times \sin(\delta) + \cos(\phi) \times \cos(\delta) \times \cos(h)] \quad (\text{degrees}) \quad (10)$$

where h is the solar hour angle at the time t from midnight

$$h = 15^\circ \times (t - 12) \quad (\text{degrees}) \quad (11)$$

$$a = \text{ArcSin}[\cos(\delta) \times \sin(h) / \sin(Z)] \quad (12)$$

Next, the filter effect of the atmosphere (OAM) must be accounted for:

$$Q_i = Q_i' \times \tau^{\text{OAM}} \quad (13)$$

$$\text{OAM} = \cos^{-1}(Z) + 1 \times 10^{-7} \quad (14)$$

Diffuse radiation is given by (Hungerford et.al., 1989):

$$q_i = q_i' \times \cos(\text{Slope}/2)^2 \quad (15)$$

where q_i' ($cal\ cm^{-2}\ min^{-1}$) is the diffuse radiation on a flat surface given by:

$$q_i' = 0.086 \times [(S \times \cos(Z))^2 \times \tau^{OAM}]^{0.5} \times (1 - S \times \cos(Z) \times \tau^{OAM})^{0.5} \quad (16)$$

Values of $LW \downarrow$ were then estimated for each weather station after calculating minimum and maximum temperatures. Atmospheric temperatures before sunrise are more homogeneous than temperatures later in the day when the sun is above the horizon, because of the surface warming process. Since the sky is assumed to be an isotropic source of $LW \downarrow$, a constant average value for $LW \downarrow$ was assumed for all the study area when minimum temperatures occurred.

At the time maximum temperatures occur, the dynamics of the atmosphere are extremely high, and atmospheric temperature is strongly influenced by surface temperature. In this case, a good linear correlation between $LW \downarrow$ and altitude was found, hence maximum temperatures were estimated and adjusted across the study area using linear regression constants calculated for each month.

Another calculation needed was the effective horizon, or the amount of hours that the sun can be seen from the slope. The potential amount of direct radiation received by a slope is determined not only by slope, aspect and angle of the receiving site, but also by the landform opposite the slope. The effective horizon was calculated using an obstruction constant (K_{obst}) that relates Q_t and radiation measured with pyranometers:

$$K_{obst} = Q_t \times \tau / (Q + q)_i \quad (17)$$

The final effect was implemented as below:

$$\tau^{(OAM-1)} = Q_t \times \cos(Z) / Q_i' \quad (18)$$

Extreme temperature interpolation

Once τ had been calculated as a function of elevation and topography properties taken from the DEM (ϕ , slope, aspect, and elevation), global solar radiation, $(Q+q)_i$, was calculated for each cell of the raster format. Although surface albedo was not measured, it was estimated to be 0.12 during the wet season and 0.15 during the dry season across the entire grid. Next, the values for $LW \downarrow$ and $LW \uparrow$ were estimated using equations 7 and 8, with the latter also used to obtain minimum and maximum temperatures.

Solar radiation interpolation

An empirical formula proposed by García (1994) was applied to compute the global solar radiation, $(Q+q)_i$. The formula was calibrated with the available solar radiation data for the study area:

$$(Q + q)_i = Q_t \times [a + b \times (T_{max} - T_{min}) / N] \quad (19)$$

where T_{max} is maximum temperature ($^{\circ}C$), T_{min} is minimum temperature ($^{\circ}C$), N is daylength (hours), $a=0.207$ and $b=0.431$.

Data

The data used to develop and test the model came from two adjacent watersheds (La Encañada and Tambomayo; approximately 16 000 ha in area) located between $7^{\circ}0'21''S$ and $7^{\circ}8'2''S$ latitude and $78^{\circ}11'22''W$ and $78^{\circ}21'31''W$ longitude. Altitude in the two watersheds varies between 2950 and 4100 m above sea level (Figure 2). The DEM was provided by the GIS Laboratory from CIP, with a resolution of 1:50 000 (De la Cruz et.al., 1999).

Daily meteorological data were obtained from three ADEFOR-CIP weather stations inside the micro-watersheds. Two new weather stations were installed in the study area during 1998 by PRONAMACHCS (Programa Nacional de Manejo de Cuencas Hidrográficas). Information provided for these stations were used as controls for validation. Further information on weather at the sites and the period of recorded data is provided in Tables 1 and 2.

RESULTS AND DISCUSSION

Maps showing the interpolated distribution of minimum temperature, maximum temperature, and solar radiation as bimonthly averages are provided in Figures 3, 4, and 5, respectively. The month of July showed the most uniformity in the distribution of minimum temperatures (Figure 3). This is because July is the middle of the dry season, hence latent heat values are low due to low moisture in the atmosphere, and net radiation fluxes are fairly homogeneous even though differences in altitude are large.

Minimum temperature distribution is more clearly related to altitude than maximum temperature. As radiation fluxes between the atmosphere and land surfaces increase during the day, a more complex relationship between the surface and atmosphere

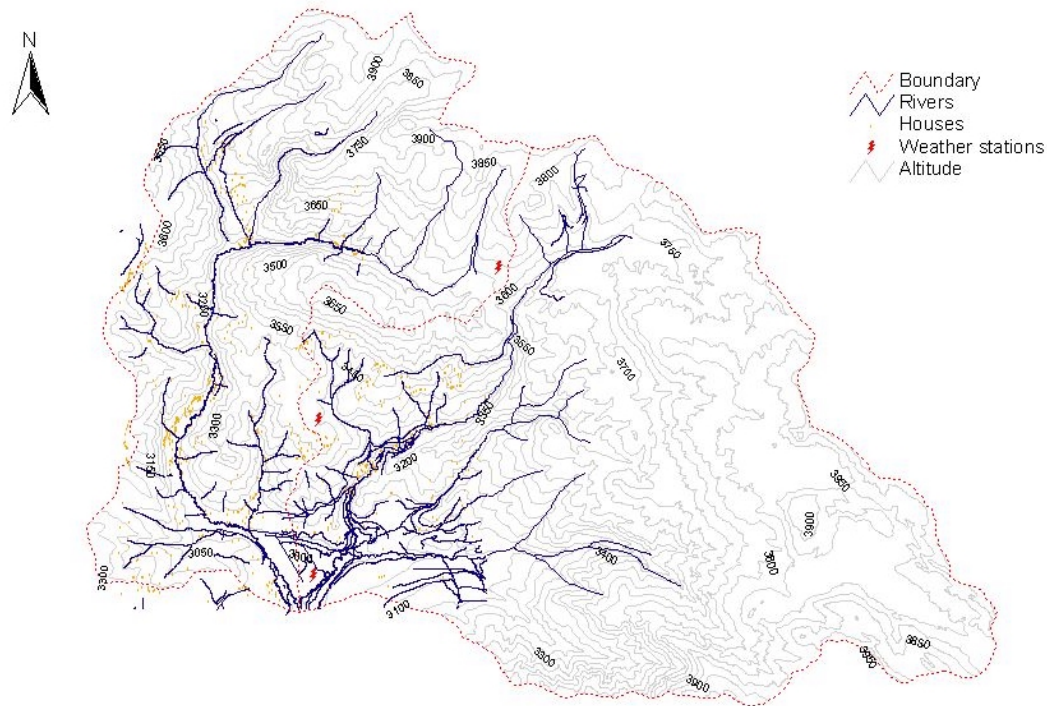


Figure 2. Digital elevation model (DEM) for the La Encañada and Tambomayo watersheds.

emerges to impact on maximum temperature calculations (Figures 3 and 4). Incoming solar radiation warms the surface thus increasing the terrestrial long-wave radiation. Important characteristics that affect ground temperature include the albedo, aspect, and slope of the surface where the solar radiation is incident. Because these characteristics vary across the landscape, maximum temperature calculations also showed high variability (Figure 4). The interpolation of maximum temperature was affected by uncertainty regarding values for surface albedo. Albedo was not measured, and the assumption that all surfaces had the same albedo was obviously not correct. The size of errors caused by uncertainty regarding albedo values will be determined in future research. One approach will be to use albedo grids provided by remote sensing or field surveys, and to increase as well the DEM resolution. To improve model accuracy, subroutines that describe the effect of albedo and soil moisture on soil temperature might be added. Surface albedo and soil water content both provide a buffer effect on the temperature.

The interpolated distribution of solar radiation depends on the spatial distribution accuracy of extreme temperature calculations. Clearly, the complex terrain in the two watersheds determined the distribution of maximum temperature and solar radiation, with both variables showing similar distributions (Figures 4 and 5). Future research will look at the use of less site-specific solar radiation routines that are more process based, but that explicitly account for the effect of slope, aspect, and effective horizon.

CONCLUSIONS

A preliminary analysis of the Climate Interpolator model has shown its utility in estimating the spatial distribution of extreme temperatures and solar radiation in complex terrain. Although the results shown here are concerned only with interpolating bimonthly averages, the same model can be used to interpolate daily values for driving soil and plant models. Daily interpolation would also be useful for

Table 1. Sources and length of records for meteorological data used to develop the interpolation techniques.

Location	Latitude (South)	Longitude (East)	Elevation (m)	Data record
Las Manzanas	-7° 7.08'	-78° 18.60'	3020	1995-1999
Usnio	-7° 5.34'	-78° 18.96'	3260	1983-1999
La Toma-Progreso	-7° 3.72'	-78° 16.92'	3590	1995-1999

Table 2. Climatological summary of data used to develop the interpolation techniques.

Weather station	Daily solar radiation (MJ m ⁻²)	Daily maximum temperature (°C)	Daily minimum temperature (°C)	Total precipitation (mm)
Las Manzanas	18.3	16.2	5.9	654.8
Usnio	19.2	14.2	6.1	707.1
La Toma-Progreso	19.9	10.8	2.8	789.5

defining the distribution of frost events across the landscape. Future research will compare interpolated estimates to measured data, and an interpolation model for rainfall will be added as well.

ACKNOWLEDGEMENTS

The authors wish to thank Mariana Cruz, Jorge de la Cruz, and Roberto Quiroz from the International Potato Center (CIP) for their technical assistance and advice in preparing the manuscript. In addition, we thank ADEFOR for the weather data.

REFERENCES

- Bonan G B (1989) A computer model of the solar radiation, soil moisture, and soil thermal regimes in boreal forest. *Ecological Modelling*, 45:275-306.
- Collins F C (1997) A Comparison of Spatial Interpolation Techniques in Temperature Estimation. [Online] Available at http://ncgia.ucsb.edu/conf-/ SANTA_FE_CD-ROM/sf_papers/collins_fred/collins.html. verified 10 Sep. 1999.
- De la Cruz J, Zorogastúa P, and Hijmans R J (1999) Atlas digital de los Recursos Naturales de Cajamarca. Departamento de Sistemas de Producción y Manejo de Recursos Naturales. Documento de Trabajo No. 2. CIP – CONDESAN. 49 p.
- Dubayah R, Rich P M (1995) Topographic solar radiation models for GIS. *Int. J. Geographical Information Systems* 9:405-419.
- García J V (1994) Principios físicos de la climatología. Ediciones UNALM. Universidad Nacional Agraria La Molina. 244 p.
- Hartkamp A D (1995) Modelling Light-interception in Mountainous Areas, Filma, an hourly sub-model for LINTUL. Report on a MSc. Thesis work. Department of Agronomy. Wageningen Agricultural University. The Netherland. 56 p.
- Hungerford R D, Nemani R R, Running S W, Coughlan J C (1989) MTCLIM: A Mountain microclimate simulation model. Research Paper INT-414. Intermountain Research Station. Forest Service. US Department of Agriculture. US. 53 p.
- Hunt L A, Boote K J (1998) Data for model operation, calibration, and evaluation. In: Tsuji, G.Y., G. Hoogenboom, and P.K. Thornton. *Understanding Options for Agricultural Production*. Kluwer Academic Publishers. pp. 9 – 40.
- Keith F, Kreider J F (1978) Principles of Solar Engineering. Hemisphere, Washington, DC, 778 p.
- Lee R (1978) *Forest Microclimatology*. Columbia University Press, New York, 276 p.
- McKenney D W, Mackey B G, Zavitz B L (1999) Calibration and sensitivity analysis of a spatially-distributed solar radiation model. *Int. J. Geographical Information Science* 13:49-65.

Peixoto J P, Oort A G (1992) Physics of Climate. American Institute of Physics. New York. US. 520 p.
Willmott C J (1996) Smart interpolation of climate variables. Third International Conference/Workshop

on Integrating GIS and Environmental Modeling. [Online]. Available at http://www.sbg.ac.at/geo/idrisi/gis_environmental_modeling/sf_papers/willmott_cort/willmott_mon1.htm. Verified 15 Dec 1999.

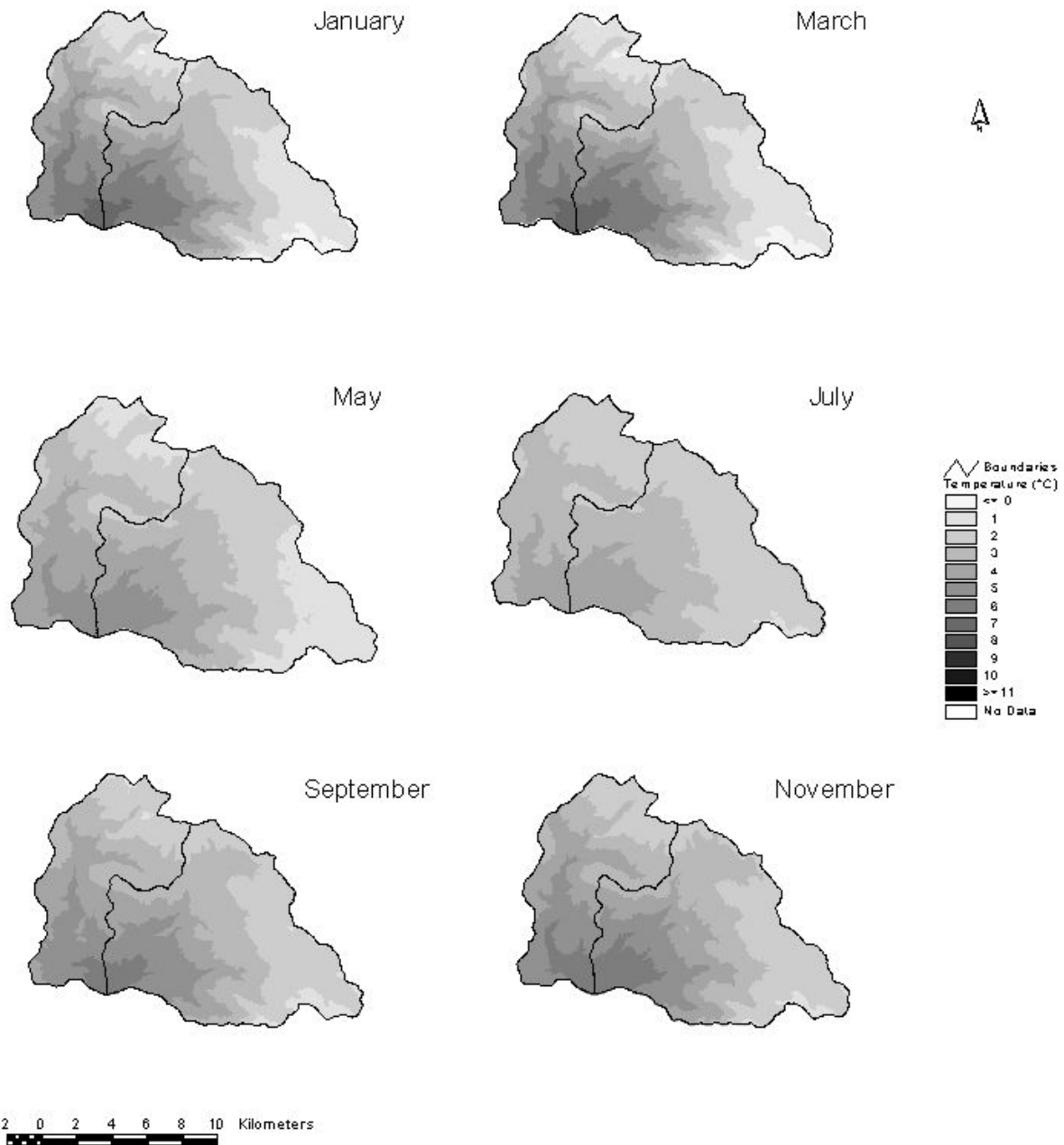


Figure 3. Interpolated distribution of minimum temperatures as bimonthly averages in the La Encañada and Tambomayo watersheds.

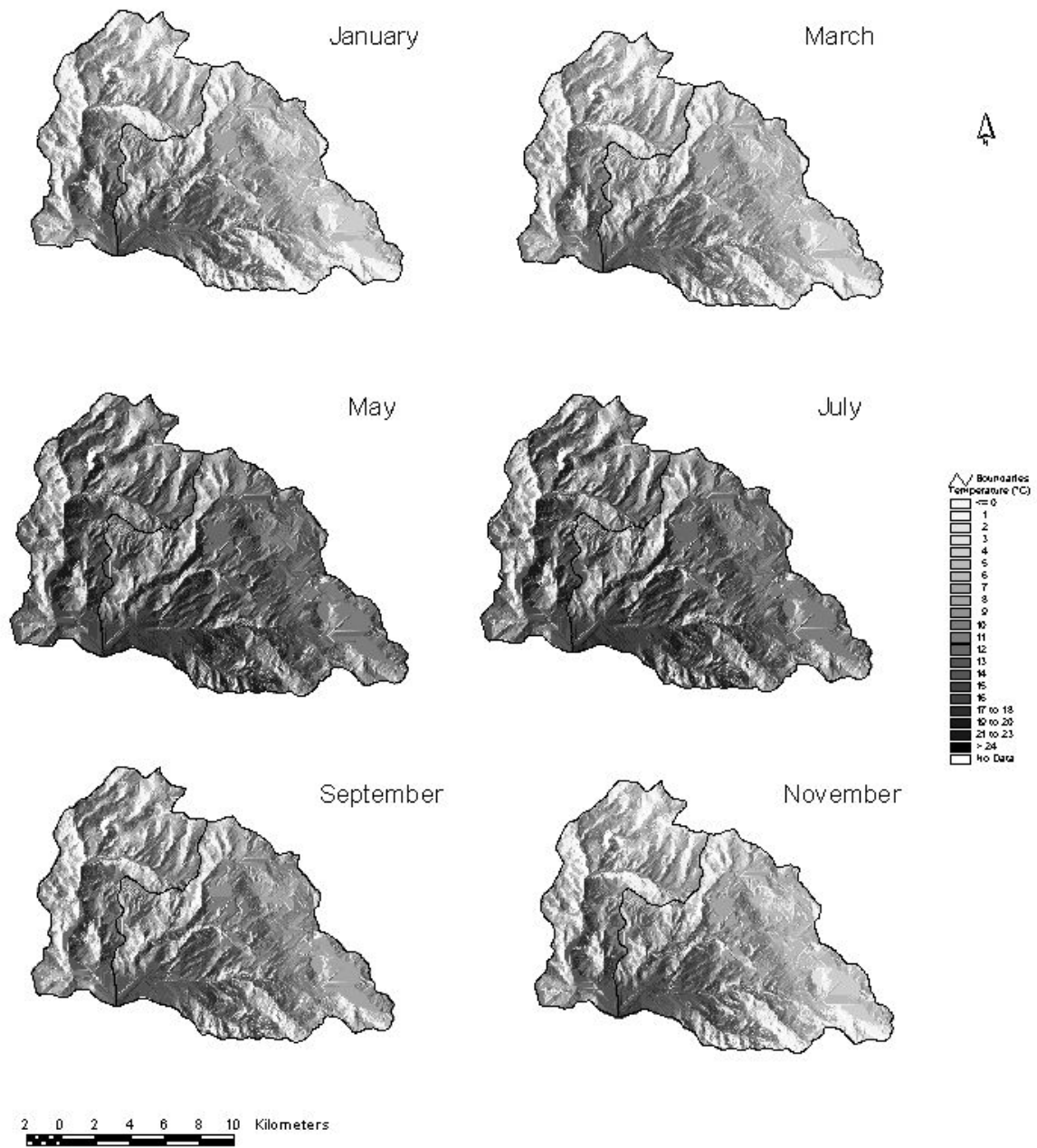


Figure 4. Interpolated distribution of maximum temperatures as bimonthly averages in the La Encañada and Tambomayo watersheds.

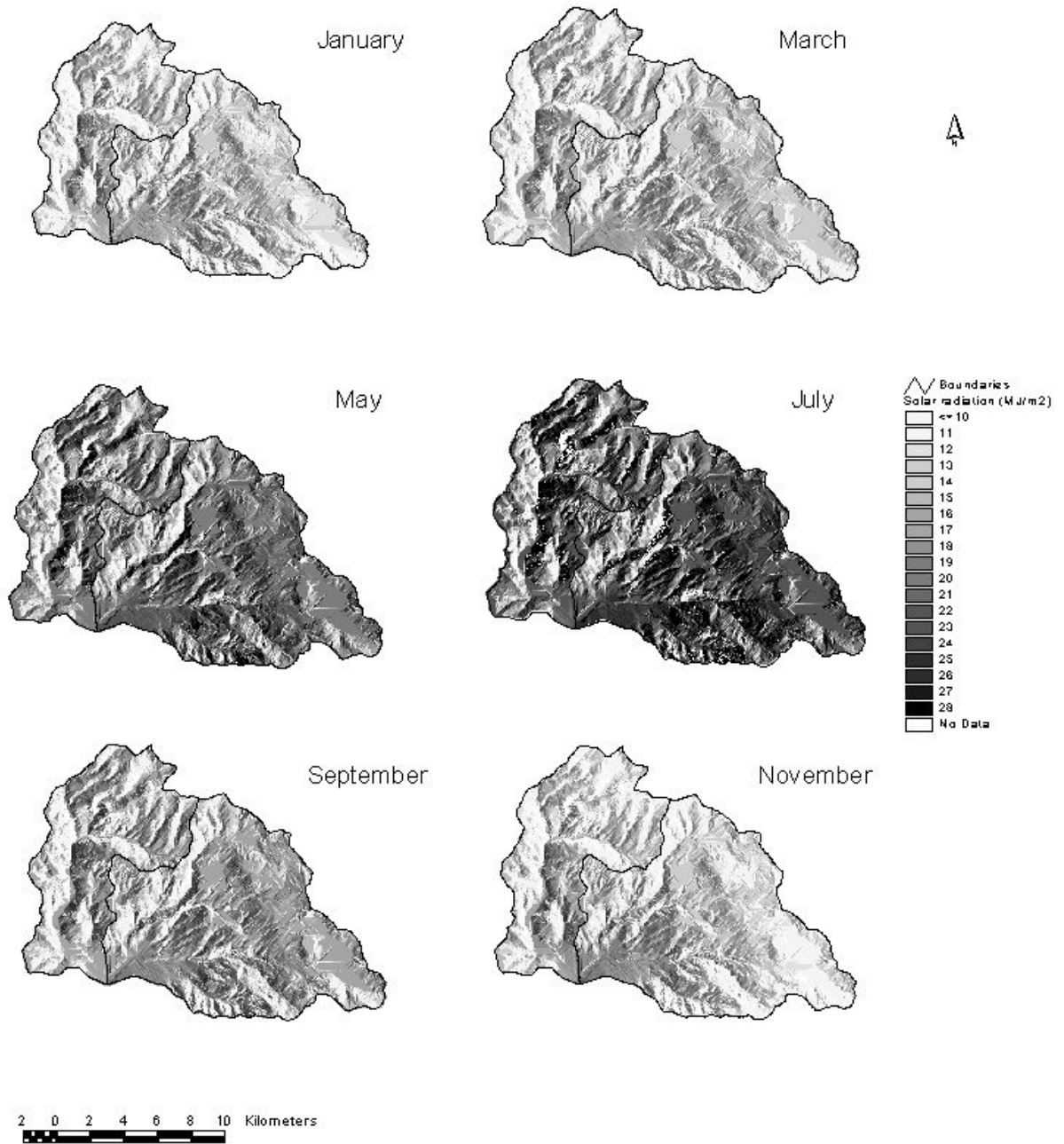


Figure 5. Interpolated distribution of solar radiation as bimonthly averages in the La Encañada and Tambomayo watersheds.